International Journal of Nanoelectronics and Materials
Volume 15 (Special Issue) March 2022 [393-404]

The Impact of Working Gas on Heat Transfer Performance of Tube Banks Heat Exchanger in a Thermoacoustic System

Chou Aw Lin[1,2], Fatimah Al Zahrah Mohd Saat[1,2,3*], Fadhliah Shikh Anuar[2,4], Mohamad Firdaus Sukri[1,2], Mohd Zaid Akop[1,2], and Patcharin Saechan[5]

[1]Fakulti Kejuruteraan Mekanikal (FKM), Universiti Teknikal Malaysia Melaka (UTeM), Hang Tuah Jaya, 76100 Durian Tunggal, Melaka, Malaysia
[2]Green and Efficient Energy Technology (GrEET), Centre for Advanced Research on Energy (CARe), Universiti Teknikal Malaysia Melaka (UTeM), Hang Tuah Jaya, 76100 Durian Tunggal, Melaka, Malaysia
[3]Centre of Excellence Geopolymer and Green Technology, Universiti Malaysia Perlis, 01000 Kangar, Perlis, Malaysia
[4]Fakulti Teknologi Kejuruteraan Mekanikal & Pembuatan (FTKMP), Universiti Teknikal Malaysia Melaka (UTeM), Hang Tuah Jaya, 76100 Durian Tunggal, Melaka, Malaysia
[5]Faculty of Engineering, King Mongkut's University of Technology North Bangkok, 10800, Bangkok, Thailand

ABSTRACT

Thermoacoustic system is a system introduced as an alternative technology for refrigerators or heat engine because it uses environmentally friendly gases as a working medium. Thermoacoustic system usually uses noble gaseous as working medium and air has been widely used since it is available abundantly and easy to handle when performing experiment. Other than air, helium is also frequently used in thermoacoustic system because its low Prandtl number is expected to improve the performance of thermoacoustic system. This paper reports the computational results of heat transfer performance across tube banks heat exchanger when air and helium are used in thermoacoustic environment. The transient cases of thermoacoustics were solved using the Shear-Stress-Transport k-ω turbulence model. The model was first validated with experimental results with air as the working fluid. The validated model was then solved for helium. Results showed that helium offers higher Nusselt number (6.52%) and Colburn-j factor (11.25%) compared to air at lower Reynolds number. Hence, the study suggests that the use of helium gas is favorable if better heat transfer is to be achieved in thermoacoustic energy system.

Keywords: CFD, heat transfer, helium gas, thermoacoustics system

1. INTRODUCTION

Environment sustainability has always been an important issue recently. Rapid development of technologies resulted in the emergence of green technologies and green energy. Research and developments on technologies have been focusing on minimizing the impact of the technologies towards the environment. Thermoacoustics was introduced as one of the green technologies in sustaining the environment. Thermoacoustics are more reliable in the perspectives of parts and components because there are no moving parts inside a thermoacoustic system, resulting in better dimensional tolerance [1]. Thermoacoustics uses noble gases as their working medium hence reducing the negative impact towards the environment [2]. There are various options for the working mediums of the thermoacoustics. Most study uses air as working medium, but helium, argon, hydrogen, and nitrogen are also some other choices that could be used as the working medium of thermoacoustics system. The choice of working medium to be used in the thermoacoustic system is important because the fluid dynamic properties of these working

*fatimah@utem.edu.my

mediums affect the thermal performance of the system since conversion of energy happens in the particles of the working medium [1].

Common thermoacoustic system consists of four basic components including a long resonator tube connected to an acoustic driver with stack (a porous media with microchannels) and heat exchanger inside the resonator tube [3]. The simplicity of the system also makes it less dimensional critical compared to conventional refrigerators and power generator [4]. The systems work by inducing the working gases to oscillate inside the resonator tube. Oscillating gases will undergo thermodynamic processes such as compression and expansion. In these thermodynamic processes, working gases carry heat and exchange heat with the working components including stacks, heat exchanger, and resonator wall [3,5,6] Hence, it can be seen that working gas plays an important factor for the performance of thermoacoustic system, because the thermal properties of working gases highly influence the thermal performance of the system [4].

Various heat transfer studies have been done in relation to thermoacoustics, however most studies use air at standard atmospheric pressure as working medium. This is probably because air at atmospheric pressure is easier to handle and is available abundantly in the open environment. Gases such as Helium are light in density, hence losses are to be expected if the system is not designed to handle the gas properly. Apart from air, gases such as helium, argon, nitrogen, and hydrogen have shown a different behaviour in fluid dynamic properties [1,7] and it was found that a better thermoacoustic performance can be obtained for gases with lower Prandtl number [1,5]. Some studies suggested that a binary mixture where the lighter gas holds a larger weightage in the mixture would help to reduce the Prandtl number [5,8]. However, regardless of binary mixture or pure monoatomic gases, the decision of gases to be used as working medium is highly dependent on the operating condition of the system due to the different performance of gases under different working condition especially under different mean pressure [1].

Helium is widely used in various studies due to its low Prandtl number, because reduction of Prandtl number is expected to increase the thermal performance of the thermoacoustic system. However, low Prandtl number sometimes might not be the only reason for selecting helium as working gas [8]. In certain working conditions and applications, the effect of helium gases has been reported to be less effective compared to other gases [9,10]. Performance of thermoacoustic system is not calculated solely based on Prandtl number, but other parameters too. Hence, it is important to understand how Prandtl number is affecting the thermal performance of heat transfer in thermoacoustic environment and analysis should also be done to understand the effect of other parameters towards thermoacoustics performance using different gases. This study focuses on the heat transfer performance in thermoacoustic environment when helium is used as the working medium. The performance of the system is presented in terms of dimensionless parameter known as Colburn-j factor.

2. METHODOLOGY

2.1 Experimental and Computational Setups

In this study, a 2-dimensional model, as shown in Figure 1, was solved for several cases using air and helium as working medium. The computational fluids dynamics model was benchmarked using experimental results of air as working medium in a quarter wavelength standing wave rig with tube banks placed at a location of approximately 0.17λ from the pressure antinode (the hard end of the resonator). The wavelength, λ, for the benchmark case was calculated to be 4.5 m and the corresponding resonance frequency of the rig is 14.2 Hz [11]. The length of the quarter wavelength resonator in the experimental setup is 6.6 m [12]. However, the computational domain was only solved for a total length of 1 meter within the tube banks area, as shown in

Figures 1 and 2. The tube banks were arranged with 9 tubes in an in-line arrangement with transverse pitch, S_T, equals the longitudinal pitch, S_L ($S_L = S_T = 45$ mm). The tube banks are made of tubes with diameter of 20 mm. In the experiment, the oscillatory flow for thermoacoustic environment was supplied by a loudspeaker (Precision Device 1860) that was controlled using an amplifier (FLP-MT1201) and a function generator (AFG 21005). The resulting velocity and temperature data were taken at two points in upstream and downstream locations of the tube banks by using the hotwire anemometer (ST-732). The measured location is as shown in Figure 2. The two locations are corresponding to a location of v_1 = 4.23 m and v_2 = 4.77 m. Type-K thermocouple was connected to a Picolog signal conditioner (TC08) to read the temperature at the upstream and downstream locations of the tube banks heat exchanger. Temperature data was taken at locations T_1 = 4.338 m and T_2 = 4.662 m, respectively. These velocity and temperature data were used to calculate the heat transfer performance. The experimental data was used for validating the computational fluid dynamics model when air is used as the working medium. The boundary conditions of the computational fluid dynamics models were set up according to the experimental set up that was used for validation of CFD model. The test section for the experimental set up is as shown in Figure 2 [12]. Fluid flow in oscillatory motion in thermoacoustic system where there is not a distinct inlet or outlet since the fluid exits and enters the system periodically. Hence, the inlet and outlet locations are denoted as x_1 and x_2 instead, as shown in Figure 1. The locations of x_1 and x_2 are 4 m and 5 m, respectively, from the pressure antinode (x = 0). User-defined functions were used at these locations of, x_1 and x_2 to induce standing wave into the system producing the thermoacoustic effects. Equation (1) and Equation (2) represent the pressure and mass flux values that were hooked at the location of x_1 and x_2, respectively. Pressure amplitude was obtained from the drive ratio as stated in Equation (3) where P_m represents the mean pressure or working pressure of the system, which is the atmospheric pressure in this case. The amplitude of pressure at the location of pressure antinode, P_a, was obtained from experimental data that was measured using a piezoresistive pressure transducer (Endevco 8510B-2) which was connected to a Dataq datalogger for data processing. The wave number is represented as k_w calculated using Equation (4) [13], frequency represented by f, and speed of sound represented by c. The operating conditions and the parameters set for boundary conditions are shown in Table 1.

$$P = P_a \cos k_w x_1 \cos(2\pi f t) \tag{1}$$

$$m' = \frac{P_a}{c} \sin k_w x_2 \cos(2\pi f t + \theta) \tag{2}$$

$$DR = \frac{P_a}{P_m} \tag{3}$$

$$k_w = \frac{2\pi f}{c} \tag{4}$$

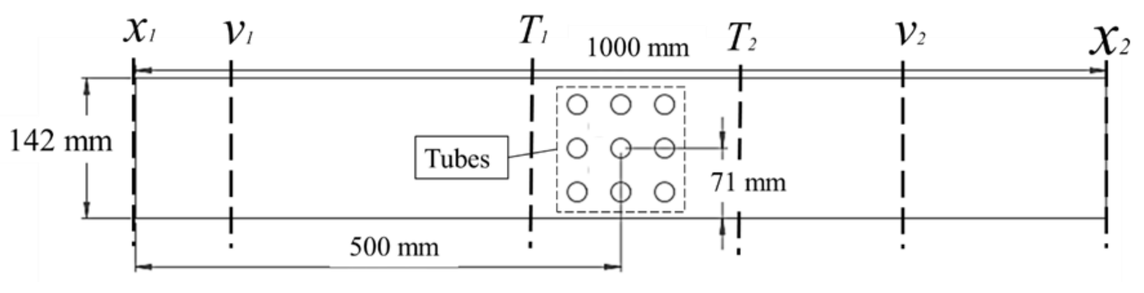

Figure 1. Geometry Modelling for CFD.

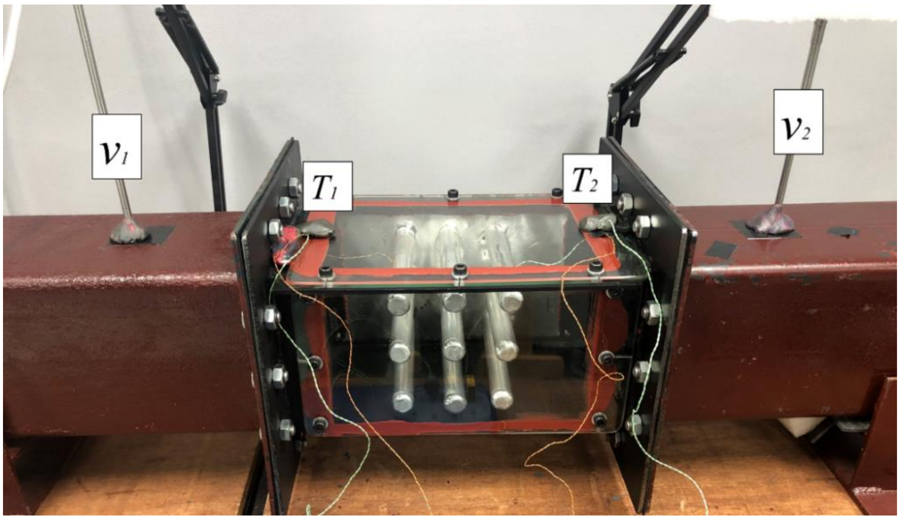

Figure 2. Experimental set up near the test section with tube banks heat exchanger.

Table 1 Operating parameters of investigated cases

	Case 1	Case 2	Case 3	Case 4	Case 5	Case 6
Working Medium	Air	Air	Air	Helium	Helium	Helium
Operating Frequency (Hz)	14.2	14.2	14.2	14.2	14.2	14.2
Tube Configuration	Inline	Inline	Inline	Inline	Inline	Inline
Surface Temperature (°C)	80	80	80	80	80	80
Drive Ratio (%)	1.22	2.17	3.11	11.31	20.00	30.00
Pressure Amplitude (Pa)	1220	2170	3110	11310	20000	30000
Mean Pressure (Pa)	100000	100000	100000	100000	100000	100000
Mass Flux (kg/m²s)	3.00	5.34	7.65	4.02	7.11	10.66

The model was solved for three different values of drive ratios and two different working media as shown in Table 1. The drive ratios that were used in the representation of the thermoacoustic flow environment is related to the parameters of flow like the velocity and the Reynolds numbers. Three drive ratios were selected where the values were selected according to the experimental values. The maximum, minimum, and average values were selected from the large range of available experimental data. These three drive ratios were tested and modelled for an inline tube banks configuration with 80°C tube surface temperature.

Grid independency test was done on the model for several element sizes to obtain the most suitable mesh for solving the model. Independency grid test was done by evaluating the changes in velocity at locations v_1 and v_2 for four different element sizes which are 0.005 m, 0.004 m, 0.003 m, and 0.002 m. Velocity data for the purpose of grid sensitivity investigation is as shown in Figure 3 for all the four element sizes. CFD models for 0.004 m, 0.003 m, and 0.002 m reported a similar velocity data. Hence, meshing with 0.003 m element size was selected for this investigation as it provides the minimum computational effort without compromising the sensitivity of the results based on the grid size.

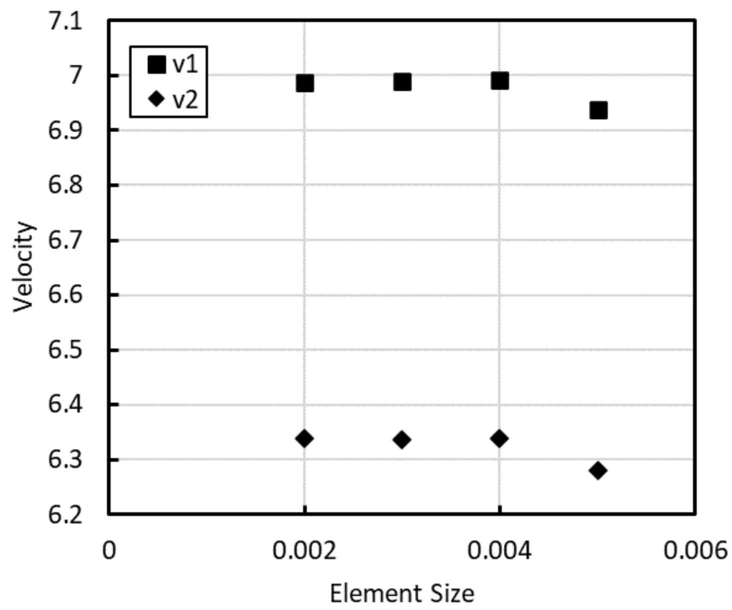

Figure 3. Grid sensitivity based on velocity for four different element sizes of mesh used in the computational domain.

2.2 Model Validation

The model was solved for 10 cycles (10000 timesteps) before data can be obtained for analysis. This is to ensure that the transient stage has reached steady stage of oscillatory flow condition. Velocity data were taken at location v_1 to be compared with velocity obtained from experimental approach. Figure 4 shows the comparison between the experimental velocity data and the CFD velocity data.

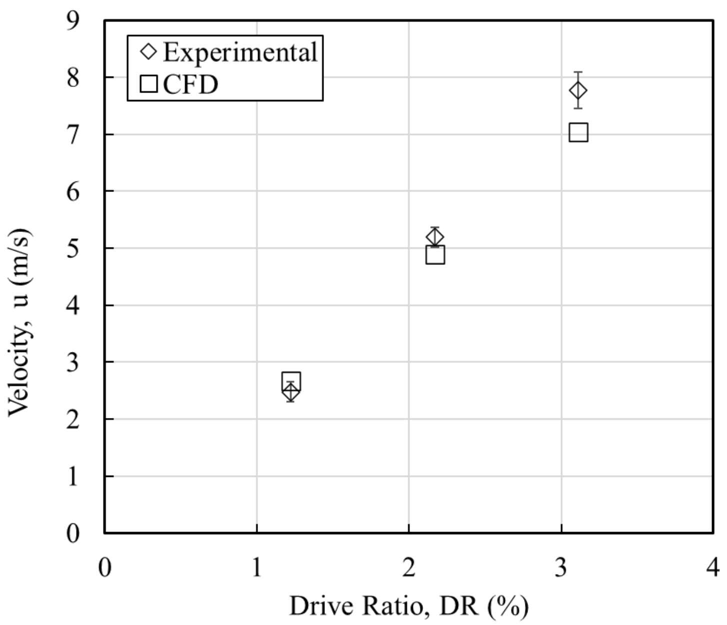

Figure 4. Validation of CFD model with experimental data.

Velocities at low drive ratio of 2.17% and 1.22% were reported with almost similar values between experiment and CFD while there is a slight difference in the case where drive ratio is 3.11%. This could be due to the unpredicted losses in the experimental rig or real-life feature that may not well be captured by the two-dimensional transient computational model. However, the reported error is small and was calculated to be approximately 9.36%. In general, the trend of changes of velocity with respect to changes of drive ratio is the same between experiment and CFD prediction. Hence, the CFD model was validated by the experimental works.
Validated model that was solved using air as working medium was then used for solving thermoacoustic flow condition with helium as the working medium. The properties of both the gaseous are as tabulated in Table 2.

Table 2 Properties of Air and Helium

	Air	**Helium**
Speed of Sound (m/s)	346	1105
Specific Heat Capacity (J/kg·K)	1.0045	5.19285
Thermal Diffusitivity (m^2/s)	2.009E-05	1.900E-04
Prandtl Number	0.7323	0.615263158

Density, ρ, of gaseous were calculated using ideal gas law as shown in Equation (5) where P, R and T are the pressure, gas constant and the temperature, respectively. The thermal conductivity of air was calculated using polynomial equation represented by Equation (6) where the coefficient of the equation was obtained from fitting the property data of air [14]. Thermal conductivity of helium on the other hand, was obtained from Equation (7). Viscosity of helium and air was calculated using Equation (8)[15] where the reference temperature, T_0 is 300K, while the viscosity reference value of μ_0 and exponent value for b_μ are as listed in Table 3 [16].

$$P = \rho R T \tag{5}$$

$$k_{Air} = 0.023635 + 7.56264 \times 10^{-5} T - 2.51537 \times 10^{-8} T^2 + 4.18521 \times 10^{-12} T^3 + 1.05973 \times 10^{-15} T^4 - 1.12111 \times 10^{-18} T^5 - 5.47329 \times 10^{-22} T^6 - 9.94835 \times 10^{-26} T^7 \tag{6}$$

$$k_{Helium} = 0.0476 + 0.362 \times 10^{-3} T + 0.618 \times 10^{-7} T^2 + 0.718 \times 10^{-11} T^3 \tag{7}$$

$$\mu = \mu_0 \left(\frac{T}{T_0}\right)^{b_\mu} \tag{8}$$

Table 3 Room Temperature Reference Values for Viscosity Equation Shown in Equation (6)

	Air	**Helium**
Reference Viscosity, μ_0 (kg/ms)	1.85×10^{-5}	1.99×10^{-5}
Viscosity Exponent, b_μ	0.76	0.68

3. RESULTS AND DISCUSSION

The results from computational models are discussed based on heat transfer performance. Both models were compared based on several parameters and the results were plotted against Reynolds number. The Reynolds number was calculated using Equation (9) [14] with hydraulic diameter defined as the diameter of the tube, D, while $\overrightarrow{v_{max}}$ represents the instantaneous maximum velocity collected at location v_1 and/or v_2. The heat transfer for helium was compared in terms of heat transfer coefficient, h, Nusselt number, Nu, and the Colburn-j factor. Heat transfer coefficient was calculated using Equation (10) where $\dot{m}$ represents mass flow rate that is calculated using Equation (11). The terms c_p, T and A_s represent specific heat capacity, temperature, and cross-sectional surface area, respectively. Nusselt number was calculated using Equation (12) where h and k represent the heat transfer coefficient and the thermal conductivity, respectively [17]. It is important to note that the temperature difference, ΔT in Equation (10) considers the temperature difference between the tube temperature and the average temperature of fluid at locations of inlet and outlet. This is because the fluid flows in an oscillatory manner in a thermoacoustic system [18, 19]. The inlet and outlet temperature values are found to be almost similar due to the cyclic nature of the flow inside the thermoacoustic system, hence considering the temperature difference between the inlet and outlet will result in a very minimal or zero heat transfer which is merely impossible. Therefore, the temperature difference is defined to be between the heated tube surface and the average temperature of fluid.

$$Re = \frac{\vec{V}_{max\,D}}{\nu} \tag{9}$$

$$h = \frac{\dot{m}c_p(\Delta T)}{A_s \Delta T_{ln}} \tag{10}$$

$$\dot{m} = \rho A_S v \tag{11}$$

$$Nu = \frac{hD}{k} \tag{12}$$

$$j = \frac{Nu}{Re\left(Pr^{1/3}\right)} \tag{13}$$

Figure 5 shows the heat transfer coefficient that was calculated and compared for different working media and the results are shown at increasing values of Reynolds number while Figure 6 shows the graph for Nusselt number that was plotted against Reynolds number. It can be seen that the heat transfer coefficient of helium is higher than that for air when the oscillatory flow of thermoacoustics is flowing across the investigated in-line tube banks heat exchanger. The gradient of increment for heat transfer coefficient with the increase of Reynolds number is higher for the case that was solved using helium as working medium. Helium has a lower density compared to air. Hence, helium is lighter, and it travels faster inside the system [20]. Low density and high velocity of helium result to an increase of mass flow rate and heat flux. As a result, heat transfer coefficient increases.

The increasing trend of Nusselt number is a result of increasing heat transfer coefficient as Reynolds number increases. However, the difference between the Nusselt number for air and that of helium is not as distinct as seen for the heat transfer coefficient. This is probably because the Nusselt number is a function of not only heat transfer coefficient, but also characteristics length and thermal conductivity. Characteristics length remains the same for air and helium since they are using the same system with the same physical descriptions. However, thermal conductivity of air is smaller compared to helium [18]. Hence, the difference in thermal conductivity between air and helium is compensating the difference that was recorded for the heat transfer coefficient of both gaseous. The Nusselt number of flow when helium is flowing at a lower Reynolds number (below 14000) was reported to be at 5.58% and 7.45% higher than air. However, in the case where Reynolds number is high, at approximately 14000, the Nusselt number of air was reported to be higher than that of helium (approximately 3.1% higher). Nusselt number, as calculated based on Equation (12), was then used to calculate the Colburn-j factor as was described in

Equation (13) [17]. Colburn-j factor is a dimensionless parameter that is represented by Nusselt number, Nu, Reynolds number, Re, and Prandtl number, Pr.

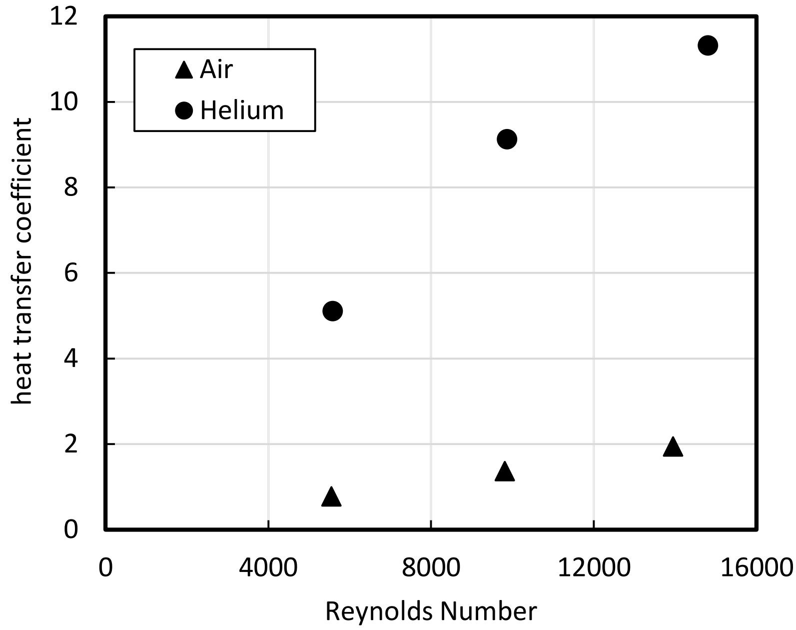

Figure 5. Comparison of heat transfer coefficient for helium and air as working medium.

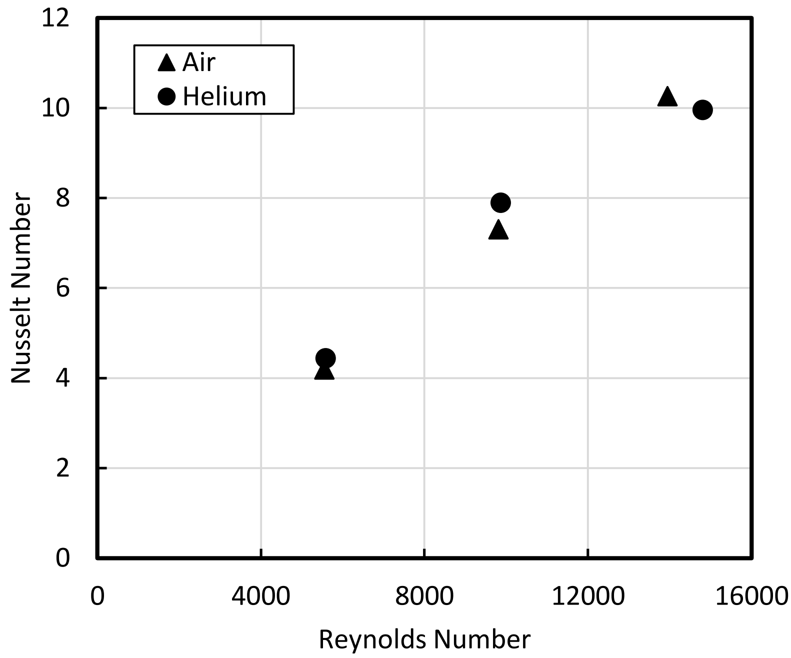

Figure 6. Comparison of Nusselt number for air and helium gas as working medium.

Figure 7 shows the variation of Colburn-j value at various Reynolds number for different working media. From Figure 7, Colburn-j values for air shows a constant decreasing trend while Colburn-j of helium seems to be similar at approximately 5000 and 10000 Reynolds number, but the value shows a significant decrease at a high Reynolds number which was a result of the Nusselt number as shown in Figure 6 when calculated against Reynolds number. This is because Colburn-j factor is a dimensionless parameter that considers the involvements of several dimensionless numbers including Reynolds number, Nusselt number, and Prandtl number. Reynolds number for air and helium are plotted at a similar range while Prandtl number of air is slightly higher compared to that of helium. It is also noted that the values of Prandtl number for both gaseous are almost constant with the increase of temperature and Reynolds number.

Considering that the Nusselt number for air is almost similar to that of the helium at a low and average Reynolds number (c.f. Figure 6), the results of Figure 7 indicates that the differences in Colburn-j values are related to the role of Prandtl number in the equation. Air has a Prandtl number that is higher than helium. The Colburn-j factor also reflects a more dominant effect of Prandtl number, showing an approximately 11.25% higher Colburn-j factor value for helium compared to air. At a higher value of Reynolds number, the Nusselt number of air can be seen to be higher than helium. In this case, helium records a Colburn-j factor of 3.29% lower compared to air. The effect of Nusselt number in this case is dominating over the effect of Prandtl number hence showing a higher Colburn-j factor of air compared to helium. The domination of the Nusselt number impact is to be expected as the convection at high Reynolds number is usually higher. The results indicate that the role of viscosity and heat capacity is important when the oscillatory flow of thermoacoustics is flowing at low Reynolds number. However, when the fluid flows with higher amplitude (higher Reynolds number), the convection is higher and therefore the Nusselt number impact is dominant.

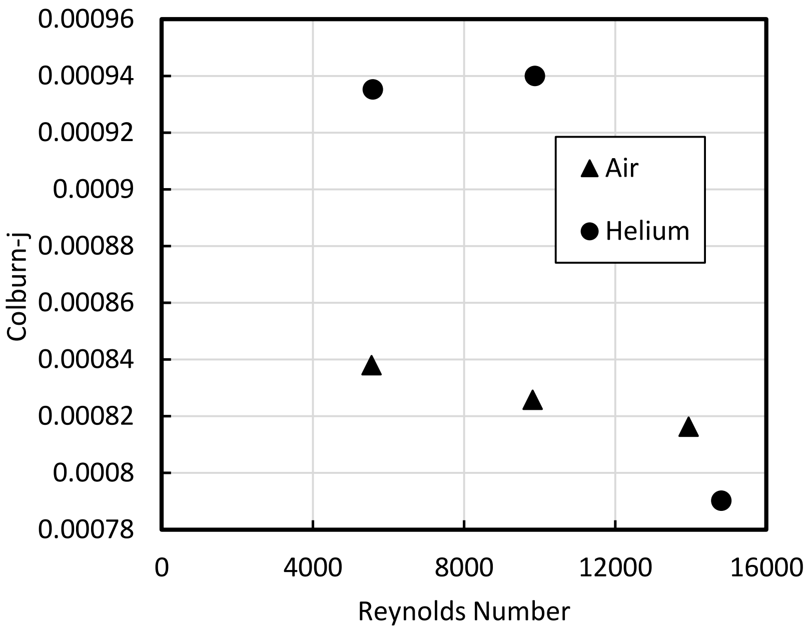

Figure 7. Comparison of Colburn-j value for air and helium as working gas.

4. CONCLUSION

Other than air, most thermoacoustic system uses helium as working medium. This study reveals the investigations that show the heat transfer performance of helium based on consideration of relevant dimensionless parameters such as Reynolds number, Prandtl number, Nusselt number and the Coburn-j factor. Results showed that helium offers a higher fluid velocity compared to air and as a result the heat transfer coefficient for helium is higher. Consequently, the Nusselt number and the Colburn-j factor of helium is higher compared to air in lower range of Reynolds number. The high thermal conductivity of helium is also affecting the Prandtl number making it low compared to air. Low Prandtl number gaseous are usually favourable in thermoacoustics as it has the ability to offer better thermoacoustic effect.

ACKNOWLEDGEMENTS

The research works were done using facilities at Universiti Teknikal Malaysia Melaka (UTeM) and are funded by the Ministry of Higher Education Malaysia under RACER/2019/FKM-CaRE/F00407.

REFERENCES

[1] Chi J., Xu J., Zhang L., Hu J., Luo E., “Study of a gas-liquid-coupled heat-driven room-temperature thermoacoustic refrigerator with different working gases,” Energy Convers. Manag., vol **246**, no. 2 (2021) article 114657, https://doi.org/ 10.1016/j.enconman.2021.114657.

[2] Shen L., Harikumar G., Wang K., and Duan F., “Flow visualization in a hybrid thermoacoustic system,” J. Acoust. Soc. Am., vol **105**, no. 5 (1999) pp. 2677-2684, https://doi.org/ 10.1016/j.expthermflusci.2021.110374.

[3] Tasnim S. H., Mahmud S., and Fraser R. A., “Modeling and Analysis of Flow, Thermal, and Energy Fields Within Stacks of Thermoacoustic Engines Filled with Porous Media,” Heat Transf. Eng., vol **34**, (2013) pp. 84-97, https://doi.org/10.1016/j.enconman.2021.114657.

[4] Dong S., Shen G., Xu M., Zhang S., and An L., “The effect of working fluid on the performance of a large-scale thermoacoustic Stirling engine,” Energy, vol. **181**, (2019) pp. 378–386, https://doi.org/10.1016/j.energy.2019.05.142.

[5] Tijani M. E. H., Zeegrs J. C. H., and Waele A. T. A. M. de, “Prandtl number and thermoacoustic refrigerators,” J. Acoust. Soc. Am., vol **112**, no. 1, (2002) pp. 134–143, https://doi.org/10.1121/1.1489451.

[6] Zhang D. W., He Y. L., Yang W. W., Wang Y., and Tao W. Q., “Particle image velocimetry measurement on the oscillatory flow at the end of the thermoacoustic parallel stacks,” Appl. Therm. Eng., vol **51**, no. 1–2, (2013) pp. 325–333, https://doi.org/10.1016/j.applthermaleng.2012.09.011.

[7] Skaria M., Rasheed K. K. A., Shafi K. A., Kasthurirengan S., and Behara U., “Influence of Working Fluid and Operating Parameters on the Performance of Traveling Wave Thermo Acoustic Prime Mover,” Int. J. Eng. Adv. Technol., no. 5, (2016) pp. 2249–8958. https://doi.org/10.1016/j.cryogenics.2011.07.004.

[8] Belcher J. R., Slaton W. V., Raspet R., Bass H. E., and Lightfoot J., “Working gases in thermoacoustic engines,” J. Acoust. Soc. Am., vol **105**, no. 5, (1999) pp. 2677–2684, https://doi.org/10.1121/1.426884.

[9] M. Chen, Y. L. Ju, “Effect of different working gases on the performance of a small thermoacoustic Stirling engine,” Int. J. Refrig., vol. **51**, (2015) pp. 41-51, https://doi.org/10.1016/j.ijrefrig.2014.12.006.

[10] B.G. Prashantha, M.S.G. Gowda, S. Seetharamu, G.S.V.L. Narasimham, "Design Analysis of Thermoacoustic Refrigerator Using Air and Helium as Working Substances," Int. J. Therm. Environ. Eng., vol. **13**, no. 2, (2017) pp. 113–120, https://doi.org/10.5383/ijtee.13.02.006.

[11] Mohd Saat F. A. Z., Johari D., and Mattokit E., “DeltaE Modelling and Experimental Study of a Standing Wave Thermoacoustic Test Rig,” J. Adv. Res. Fluid Mech. Therm. Sci., vol **60**, Issue 2, (2019) pp. 155-165.

[12] Hasbullah N., Moha Saat F. A. Z., Anuar F. S., Johari D., and Sukri M. F., “Temperature and velocity changes across tube banks in one-directional and bi-directional flow conditions,” Evergreen, vol **8**, no. 2, (2021) pp. 428–437, https://doi.org/10.5109/4480725.

[13] Kamsanam W., Mao X., and Jaworski A. J., “Thermal performance of finned-tube thermoacoustic heat exchangers in oscillatory flow conditions,” Int. J. Therm. Sci., vol **101**, (2016) pp. 169–180, https://doi.org/10.1016/j.ijthermalsci.2015.10.032.

[14] Y.A. Cengel, A.J. Ghajar, "Heat and mass transfer: Fundamentals and applications," 5th ed. New York, NY: McGraw-Hill Professional, (2014) pp. 934.
[15] Vargaftik N. B., and Yakush L. V., "Temperature dependence of thermal conductivity of helium," J. Eng. Phys., vol **32**, no. 5, (1977) pp. 530–532.
[16] G. W. Swift, "Thermoacoustics: A Unifying Perspective for Some Engines and Refrigerators," 2nd ed. Cham: Springer International Publishing, (2017) pp. 49.
[17] Kamsanam W., Mao X., and Jaworski J., "Development of experimental techniques for measurement of heat transfer rates in heat exchangers in oscillatory flows," Exp. Therm. Fluid Sci., vol **62**, (2015) pp. 202–215, https://doi.org/10.1016/j.expthermflusci.2014.12.008.
[18] Hasbullah N., Mohd Saat F.A.Z, Shikh Anuar F., Sukri M.F., Saechan P., "Experimental and numerical studies of one-directional and bi-directional flow conditions across tube banks heat exchanger," Therm. Sci. Eng. Prog., vol **28**, (2022) pp. 101176, https://doi.org/10.1016/j.tsep.2021.101176.
[19] Allafi W.A., Mohd Saat F.A.Z., Mao X., "Fluid dynamics of oscillatory flow across parallel-plates in standing-wave thermoacoustic system with two different operation frequencies". Int. J. Eng. Sci. Technol., 24, (2021), pp 41-49.https://doi.org/10.1016/j.jestch.2020.12.008
[20] Prashantha B. G., Gowda M. S. G., Seetharamu S., and Narasimham G. S. V. L., "Design Analysis of Thermoacoustic Refrigerator Using Air and Helium as Working Substances," Int. J. Therm. Environ. Eng., vol **13**, no. 2, (2017) pp. 113–120, https://doi.org/10.5383/ijtee.13.02.006.

NOMENCLATURE

A_S	Cross-sectional Area, m^2
CFD	Computational Fluid Dynamics
c	speed of sound, $m \cdot s^{-1}$
c_p	Specific heat capacity, $kJ \cdot kg^{-1} \cdot K^{-1}$
D	Hydraulic diameter, m
f	frequency, hz
h	Heat transfer coefficient, $W \cdot m^{-2} \cdot K^{-1}$
j	Colburn-j factor
k	Thermal conductivity, $W \cdot m^{-1} \cdot K^{-1}$
k_w	wave number, m^{-1}
$\dot{m}$	Mass flow rate, $kg \cdot s^{-1}$
m'	Mass flux, $kg \cdot s^{-1} \cdot m^{-2}$
Nu	Nusselt number
P	pressure, kPa
Pr	Prandtl number
R	gas constant, $J \cdot K^{-1} \cdot mol^{-1}$
Re	Reynolds Number
S	Pitch, mm
T	temperature, K
v	velocity, $m \cdot s^{-1}$
x	distance from antinode, m
θ	Phase angle, rad
λ	Wavelength, m
μ	Dynamic Viscosity, $kg \cdot m^{-1} \cdot s^{-1}$
π	3.14159
ρ	Density, $kg \cdot m^{-3}$

Subscript

1	Location 1
2	Location 2
a	amplitude
L	longitudinal
ln	log mean value of temperature difference
m	mean
max	maximum
t	transverse